Density-matrix spectra of solvable fermionic systems

Ming-Chiang Chung and Ingo Peschel
Fachbereich Physik, Freie Universität Berlin, Arnimallee 14, D-14195 Berlin, Germany
(Received 14 March 2001; published 23 July 2001)

We consider noninteracting fermions on a lattice and give a general result for the reduced density matrices corresponding to parts of the system. This allows to calculate their spectra, which are essential in the density-matrix renormalization group method, by diagonalizing small matrices. We discuss these spectra and their typical features for various fermionic quantum chains and for the two-dimensional tight-binding model.

DOI: 10.1103/PhysRevB.64.064412 PACS number(s): 75.10.Jm, 05.30.−d

I. INTRODUCTION

Density matrices have found an interesting application in recent years. In the density-matrix renormalization group (DMRG) method[1–3] a quantum system is built from smaller parts and the idea is to work with basis functions in these parts which are optimal for the combined system. These are the eigenfunctions of the reduced density matrices which have the largest eigenvalues w_n. Obviously, the procedure will work well if the eigenvalue spectrum drops rapidly, such that a small number of functions practically exhausts the sum rule $\Sigma w_n = 1$. For quantum chains this is indeed the case. The numerical calculations show a roughly exponential decrease of the eigenvalues.[2,4] Of course, this raises the question whether such spectra can be obtained explicitely for some solvable models. For noncritical systems this is possible by using the relation[5] between the density matrices of quantum chains and the corner transfer matrices[6] (CTM's) of the corresponding two-dimensional classical problems. In this way, the spectra for the transverse Ising chain,[7] the XXZ Heisenberg chain,[7] and a chain of coupled oscillators[8] could be determined in the thermodynamic limit and compared with DMRG calculations. In all these cases, one finds simple analytic expressions and, apart from degeneracies, a strictly exponential behavior. This does not hold for the chiral three-state Potts chain[9] or for nonintegrable models,[10,11] but qualitatively the spectra are similar.

Given the importance of fermionic systems in general and also for DMRG applications, one would of course like to have results for this case, too. The transverse Ising chain can be viewed as a fermionic model, but the CTM approach does not make use of this and is limited to large noncritical systems. Therefore an alternative approach is necessary by which one can treat solvable fermion systems of arbitrary size. In the present communication we show how this can be done. The systems which we consider are noninteracting, such that the Hamiltonian can be diagonalized by a Bogoliubov transformation. Using an explicit form of the state in question (usually the ground state), we show that arbitrary reduced density matrices can be calculated exactly and have the general form $\exp(-\mathcal{H})$. The operator $\mathcal{H}$ describes a collection of noninteracting fermions with single-particle eigenvalues ε_l. Apart from the different statistics, this is the same situation as for coupled oscillators.[8,12] The ε_l, which determine the properties of the spectrum, follow from the eigenvalues of an $M \times M$ matrix, where M is the number of sites in the chosen subsystem. In general, they have to be calculated numerically. One should stress that the dimensionality of the system plays no essential role.

In the following Sec. II we sketch the general method of computation which uses coherent fermionic states for calculating the necessary partial traces. In Sec. III, we apply it to the transverse Ising chain and discuss the resulting spectra for a number of situations, including the critical case, the first excited state and related row transfer matrices. Section IV deals briefly with another one-dimensional problem, namely the spin one-half XY chain in a field. This is interesting because it has a disorder point where the spectrum collapses. In Sec. V we turn to the physically most important case of a tight-binding model which we dicuss in two dimensions. We present spectra for systems of various sizes and shapes, as well as truncation errors showing the difficulties in this case. Section VI, finally, contains a summary and some additional remarks. Some technical details can be found in the Appendix.

II. METHOD

We consider Hamiltonians which are quadratic in Fermi operators and thus have the general form

$$H = \sum_{ij=1}^{L} \left[c_i^\dagger A_{ij} c_j + \frac{1}{2}(c_i^\dagger B_{ij} c_j^\dagger + \text{H.c.}) \right], \tag{1}$$

where the c_i's and $c_i^\dagger$'s are Fermi annihilation and creation operators. Because of the Hermiticity of H, the matrix $\mathbf{A}$ is Hermitian and $\mathbf{B}$ is antisymmetric. In the following we consider only real matrices. One can diagonalize H through the canonical transformation[13]

$$\eta_k = \sum_i (g_{ki} c_i + h_{ki} c_i^\dagger), \tag{2}$$

which leads to

$$H = \sum_k \Lambda_k \eta_k^\dagger \eta_k + \text{const.} \tag{3}$$

The quantities Λ_k^2 are the eigenvalues of the matrices $(\mathbf{A}-\mathbf{B})(\mathbf{A}+\mathbf{B})$ and $(\mathbf{A}+\mathbf{B})(\mathbf{A}-\mathbf{B})$, the corresponding eigenvectors being $\phi_{ki} = g_{ki} + h_{ki}$ and $\psi_{ki} = g_{ki} - h_{ki}$, respectively.

Consider now the ground state $|\Phi_0\rangle$ of the Hamiltonian (1) for an even number of sites L. Due to the structure of H,

it is a superposition of configurations with either an even or an odd number of fermions. This suggests to write it (for the even case) in the form

$$|\Phi_0>=C\exp\left\{\frac{1}{2}\sum_{ij}\ G_{ij}c_i^\dagger c_j^\dagger\right\}|0\rangle, \tag{4}$$

where $|0\rangle$ is the vacuum of the c_i, i.e.,

$$c_i|0\rangle=0. \tag{5}$$

Such an exponential form is known from superconductivity, where the BCS wave function (in momentum space) can be written in this way. [14]

One obtains G_{ij} by applying the Fermi operators η_k to the ground state

$$\eta_k|\Phi_0\rangle=0 \quad \text{for all } k, \tag{6}$$

which leads to (see Appendix)

$$\sum_m\ g_{km}G_{mn}+h_{kn}=0 \quad \text{for all } k,n. \tag{7}$$

Thus **G** relates the two matrices **g** and **h** of the transformation (2). Using Eq. (4), one obtains the total density matrix $\rho_0=|\Phi_0\rangle\langle\Phi_0|$ explicitly in an exponential form

$$\rho_0=|C|^2\exp\left(\frac{1}{2}\sum_{ij}\ G_{ij}c_i^\dagger c_j^\dagger\right)|0\rangle\langle 0|\exp\left(-\frac{1}{2}\sum_{ij}\ G_{ij}c_ic_j\right). \tag{8}$$

One now divides the total system in two parts (system and environment in the DMRG terminology) and looks for the reduced density matrix in part 1. This is obtained by taking the trace over part 2:

$$\rho_1=\mathrm{Tr}_2(\rho_0). \tag{9}$$

In order to calculate ρ_1, one uses the fermionic coherent states defined by[15]

$$c_i|\xi_1\cdots\xi_L\rangle=\xi_i|\xi_1\cdots\xi_L\rangle. \tag{10}$$

Such states can be built from the vacuum with operators c_i and Grassmann variables ξ_i

$$|\xi_1\cdots\xi_L\rangle=\exp\left(-\sum_i\ \xi_ic_i^\dagger\right)|0\rangle. \tag{11}$$

Using this, one can write the trace of an operator O as

$$\mathrm{Tr}\,O=\int\prod_\alpha\ d\xi_\alpha^*d\xi_\alpha e^{-\sum_\alpha\ \xi_\alpha^*\xi_\alpha}\langle-\xi|O|\xi\rangle. \tag{12}$$

After forming a general matrix element of ρ_0 with such states and taking the trace over the environment with Eq. (12), one obtains, if part 1 consists of M sites

$$\begin{aligned}\langle\xi_1\cdots\xi_M|\rho_1|\xi_1'\cdots\xi_M'\rangle&=|C|^2\int\prod_{i=M+1}^{L}\ d\xi_i^*d\xi_ie^{-\sum_i\ \xi_i^*\xi_i}\langle\xi_1\cdots\xi_M\\&\quad-\xi_{M+1}\cdots-\xi_L|\rho_0|\xi_1'\cdots\xi_M'\xi_{M+1}\cdots\xi_L\rangle.\end{aligned} \tag{13}$$

Inserting Eq. (8) leads to an integrand which contains only quadratic forms of Grassmann variables in the exponents. The integration can then be carried out by rotating and displacing the variables as for a Gaussian integral with complex numbers. This gives

$$\begin{aligned}\langle\xi_1\cdots\xi_M|\rho_1|\xi_1'\cdots\xi_M'\rangle&=|C|^2\exp\left(\sum_{ij}\ \alpha_{ij}\xi_i^*\xi_j^*\right)\exp\left(\sum_{ij}\ \beta_{ij}\xi_i^*\xi_j'\right)\\&\quad\times\exp\left(-\sum_{ij}\ \alpha_{ij}\xi_i'\xi_j'\right),\quad i,j\leqslant M.\end{aligned} \tag{14}$$

The $M\times M$ matrices α and β appearing here are defined as follows. One divides **G** into four submatrices a^{11}, a^{12}, a^{21}, and a^{22}, according to whether the sites i,j belong to part 1 or part 2. In terms of these

$$\begin{aligned}2\alpha&=a^{11}+ca^{22}c^T,\\\beta&=cc^T,\end{aligned} \tag{15}$$

where $c=a^{12}(1-a^{22})^{-1}$ and c^T denotes its transpose. As shown in the Appendix one can reconstruct the operator form of ρ_1 from the matrix elements (14) . This gives

$$\begin{aligned}\rho_1&=|C|^2\exp\left(\sum_{ij}\ \alpha_{ij}c_i^\dagger c_j^\dagger\right)\exp\left(\sum_{ij}\ (\ln\beta)_{ij}c_i^\dagger c_j\right)\\&\quad\times\exp\left(-\sum_{ij}\ \alpha_{ij}c_ic_j\right),\quad i,j\leqslant M.\end{aligned} \tag{16}$$

Finally, since the Fermi operators appear quadratic in the exponents, ρ_1 can be diagonalized with a Bogoliubov transformation as in Eq. (2). As a result,

$$\rho_1=K\exp\left(-\sum_{l=1}^{M}\ \varepsilon_lf_l^\dagger f_l\right) \tag{17}$$

with new Fermi operators $f_l^\dagger, f_l$ and $K=|C|^2$. The single-particle eigenvalues ε_l follow from the matrices α,β according to Eq. (A9) of the Appendix. The normalization factor K is fixed by the sum rule $\mathrm{Tr}(\rho_1)=1$. In this way, one can calculate the density-matrix spectra numerically for an arbitary part of a finite system with Hamiltonian (1).

III. TRANSVERSE ISING CHAIN

As a first example,we consider in this section the transverse Ising chain with open boundaries described by

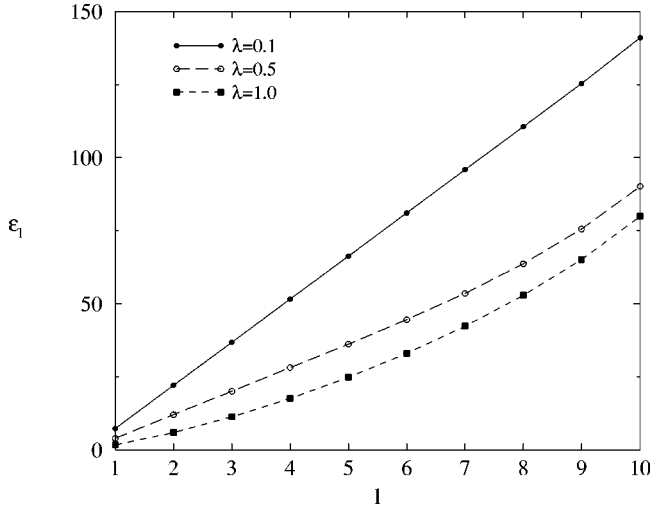

FIG. 1. Single-particle eigenvalues ε_l for one-half of a transverse Ising chain, arranged in ascending order. The system is in the ground state, $L=20$ and $\lambda<1$.

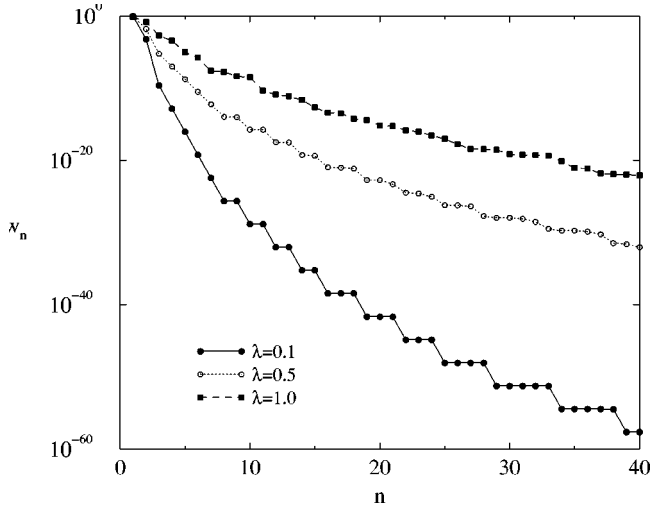

FIG. 2. Density-matrix eigenvalues w_n, arranged in decreasing order, obtained from the ε_l in Fig. 1 and for the same parameters.

$$H=-\sum_{i=1}^{L}\sigma_i^z-\lambda\sum_{i=1}^{L-1}\sigma_i^x\sigma_{i+1}^x, \tag{18}$$

where the σ^α are Pauli spin matrices and the transverse field has been set equal to one. In the thermodynamic limit, this system has a quantum critical point at $\lambda=1$ and long-range order in σ^x for $\lambda>1$. In terms of spinless fermions H reads

$$H=-2\sum_{i=1}^{L}(c_i^\dagger c_i-1/2)-\lambda\sum_{i=1}^{L-1}(c_i^\dagger-c_i)(c_{i+1}^\dagger+c_{i+1}) \tag{19}$$

and thus has the form (1). In the following we discuss the reduced density matrix ρ_1 for one half of the chain, i.e., $M=L/2$.

We first consider the ground state. In Fig. 1, the single-particle eigenvalues ε_l are plotted for $L=20$ and different coupling constants λ. For $\lambda=0.1$ they all lie on a straight line, which corresponds to the situation one finds in the thermodynamic limit. This is what one expects since the correlation length is much less than L and hence boundary effects should be small. One can also check that the values are exactly those obtained analytically via corner transfer matrices.[7] It seems to be difficult, however, to derive these results directly from our equations. For larger coupling, $\lambda=0.5$, only the first ε_l follow a linear law, then the curve bends upwards. This is similar to the behavior one finds for finite-size corner transfer matrices,[16] although the geometry there is different. At the same time, the initial slope decreases. Finally, at the critical point, the whole graph is curved. In the ordered region (not shown), a linear regime develops again.

From the ε_l one obtains the actual eigenvalues w_n of ρ_1 by specifying the occupation numbers $f_l^\dagger f_l$ in Eq. (17). The resulting spectra are shown in Fig. 2 in a semi-logarithmic plot. Note that not all w_n are shown, however they are correctly normalized to one. Similar results, but for a smaller number of w_n, were obtained in Ref. 7 via DMRG calculations. Due to the relatively large values of the ε_l there is a rather rapid decay (note the vertical scale) so that the system can be treated very well by DMRG.[17,18] This holds even at the critical point, where the decay is slowest.

The situation there is presented in more detail in the next figures. Figure 3 shows the ε-spectra for various sizes of the system. As L increases, the number of ε increases, the curves become flatter, but the curvature remains. There is no sign of a linear region related to conformal invariance on this scale (compare Ref. 16). The w_n spectra are plotted in Fig. 4. Because of the form of the ε, there are few degeneracies and the curves have the typical, relatively smooth shape found also for other critical systems.[2,4] The finite-size effects show up essentially in the tails.

So far, we have treated the ground state, but one can also determine the density matrices for the first excited state $|\Phi_1\rangle$. This state contains an odd number of fermions. To apply the formalism here, one can perform a particle-hole

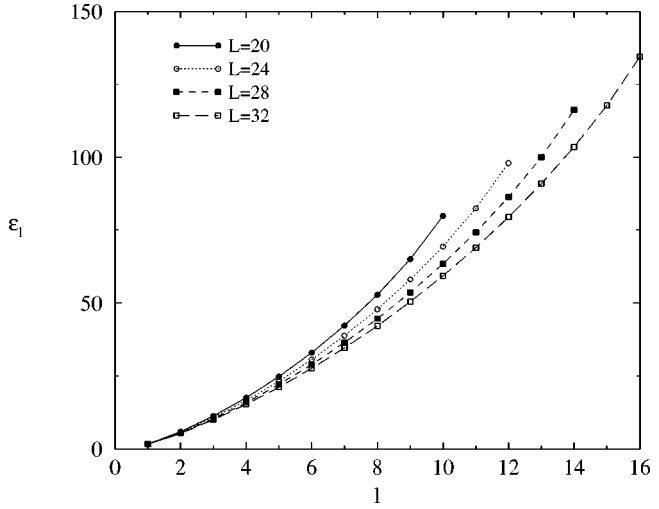

FIG. 3. Single-particle eigenvalues ε_l for critical transverse Ising chains in the ground state.

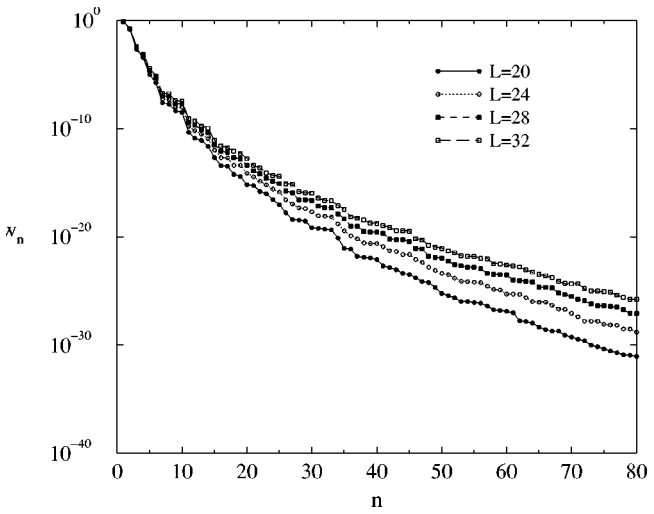

FIG. 4. Density-matrix eigenvalues w_n for transverse Ising chains at the critical point obtained from the ε_l in Fig. 3.

transformation at one site, e.g., $c_1^\dagger \leftrightarrow c_1$. Then $|\Phi_1\rangle$ appears in the even subspace and can be written in the form (4). With the help of the relations

$$\eta_1^\dagger |\Phi_1\rangle = 0,$$

$$\eta_k |\Phi_1\rangle = 0 \quad \text{for} \quad k \geq 2, \tag{20}$$

one can then derive the corresponding equation for the matrix G_{ij}. In this way, the single-particle eigenvalues ε_l shown in Fig. 5 were obtained. In contrast to the case of the ground state, the first eigenvalue is zero here. This reflects the fact that, in the original representation, the fermion number is odd, while the number of sites is even. The other eigenvalues are very similar to those for the ground state. In particular, one has a linear spectrum away from $\lambda = 1$ and a curved one at the critical point. The vanishing ε_1 causes all eigenvalues w_n of ρ_1 to be at least doubly degenerate.

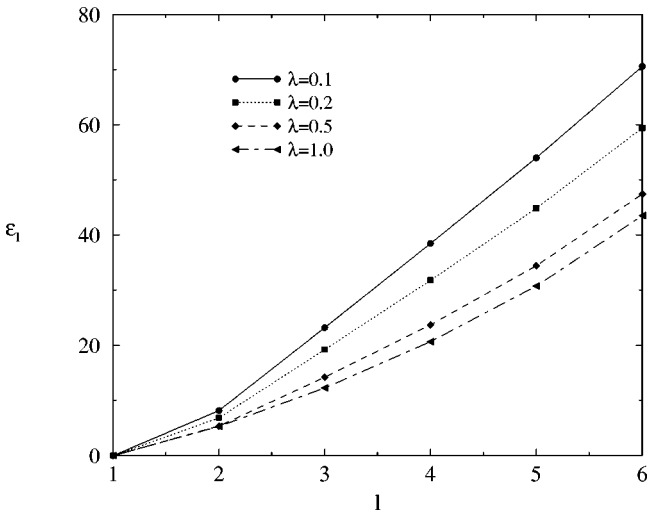

FIG. 5. Single-particle eigenvalues ε_l for the first excited state of a transverse Ising chain for $L=12$ and four values of λ.

Finally, the closely related problem of the row-to-row transfer matrices for the two-dimensional Ising model can be studied in the same way. For a square lattice with couplings K_1 (K_2) in the vertical (horizontal) direction one can consider two symmetrized versions, namely

$$V = V_2^{1/2} V_1 V_2^{1/2}, \quad W = V_1^{1/2} V_2 V_1^{1/2}, \tag{21}$$

where V_1 (V_2) contain the vertical (horizontal) bonds. Both represent fermionic quantum chains and can be diagonalized also for open boundaries.[19,20] For the thermodynamics, one needs the eigenvector with maximal eigenvalue. DMRG calculations using the operator V have already been done.[21] The spectrum of the ε_l in the isotropic case $K_1 = K_2$ is very similar to that found above in Fig. 1. This also holds for the magnitude of the ε_l and the problem can therefore be treated equally well by DMRG. For W the ε-spectrum is strictly linear at the lower end and described by a formula containing elliptic integrals as in Ref. 7, while for V the values are somewhat smaller and there is a deviation from linearity for the first ε_l. This reflects the difference in the representation of ρ_1 via CTM's in the two cases.

IV. *XY*-SPIN CHAIN

In this section we consider briefly the spin one-half quantum chain described by the Hamiltonian

$$H = -J/2 \sum_{i=1}^{L-1} [(1+\gamma)\sigma_i^x \sigma_{i+1}^x + (1-\gamma)\sigma_i^y \sigma_{i+1}^y + h(\sigma_i^z + \sigma_{i+1}^z)], \tag{22}$$

which reads in terms of fermions

$$H = -J \sum_{i=1}^{L-1} [(c_i^\dagger c_{i+1} + \gamma c_i^\dagger c_{i+1}^\dagger + \text{H.c.}) + h(c_i^\dagger c_i + c_{i+1}^\dagger c_{i+1} - 1)]. \tag{23}$$

Although similar to the transverse Ising chain, this system has a special feature. For

$$\gamma^2 + h^2 = 1 \tag{24}$$

the ground state simplifies and also becomes twofold degenerate. In the spin language, one has two simple product states.[22] Moreover, the behavior of correlation functions changes from monotonic to oscillatory[23] and thus Eq. (24) represents a "disorder line."[24] On this line, H describes also a stochastic reaction-diffusion model[25] equivalent to Glauber's kinetic spin model.

The appearance of a simple ground state can be observed in the density-matrix spectrum and has already been seen in DMRG calculations for certain other models (see Sec. 3.1 in Ref. 3). For the XY chain, it can be investigated very well in the fermionic approach.

In Fig. 6 we show the lowest ε_l values as a function of the parameter h for fixed $\gamma = 1/2$. The disorder point according to Eq. (24) is then at $h_0 = 0.866$. One can see that, coming from larger values of h, all ε_l except the lowest one diverge as one

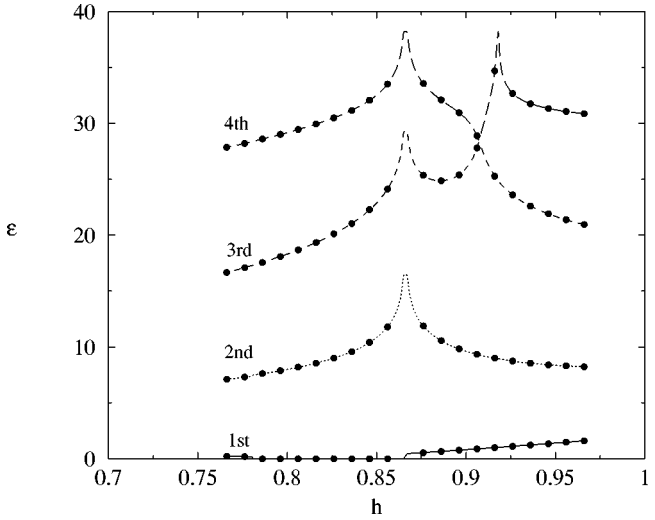

FIG. 6. The four lowest single-particle eigenvalues ε for an XY spin chain in a field h. The anisotropy is $\gamma=0.5$, the length $L=8$. Lines result from the analytical method, solid circles from a DMRG calculation.

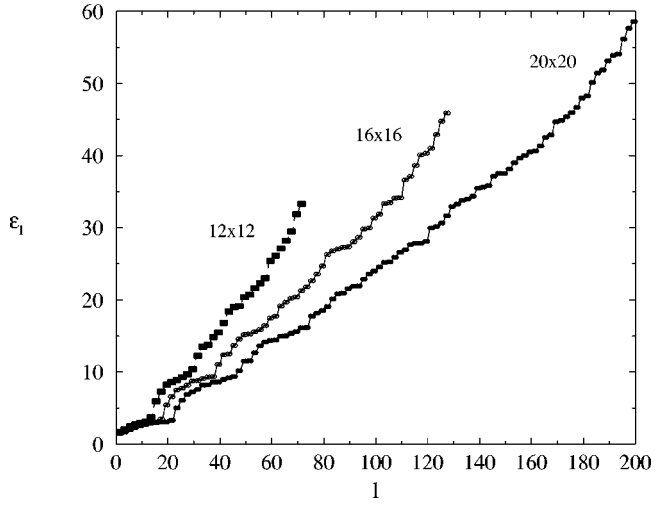

FIG. 7. Single-particle eigenvalues ε_l for two-dimensional tight-binding models of different sizes. The ε_l are for one-half of the system.

approaches h_0. For $h<h_0$ they become finite again. In this region, however, one has to work in another subspace since at h_0 the lowest fermionic eigenvalue Λ_0 in H crosses zero, which leads to the degeneracy of the ground state. This can be done as for the excited state in Sec. III. Then one finds the curves in the figure. As a check we also performed direct DMRG calculations and found complete agreement (dots). Such crossings appear repeatedly as one reduces h further. The next one (for the chosen L) takes place at $h=0.78$. However, as seen from the figure, the higher ε_l show no effects at this point, indicating that the ground state of H does not simplify there. At h_0, the divergence of the ε_l for $l\geqslant 2$ together with the value $\varepsilon_1=0$ lead to the density-matrix eigenvalues $w_1=w_2=1/2$, while all other w_n are zero, i.e., the spectrum collapses at this point. This effect could be a tool in the search for simple ground states by DMRG.

V. TWO-DIMENSIONAL TIGHT-BINDING MODEL

As the last, but most important example we consider a tight-binding model with open boundaries described by

$$H=-\sum_{\langle \mathbf{i},\mathbf{j}\rangle}(c_{\mathbf{i}}^{\dagger}c_{\mathbf{j}}+c_{\mathbf{j}}^{\dagger}c_{\mathbf{i}}), \tag{25}$$

where the brackets $\langle \mathbf{i},\mathbf{j}\rangle$ denote nearest-neighbor sites. This model is critical and solvable in all dimensions. We treat it here for the case of a square lattice and we assume that the system also has the shape of a square with $L=N^2$ sites where N is even. This problem has served as a DMRG test case some time ago.[26]

The ground state here is different from that in the previous sections. Because H only contains hopping, $B=0$ in Eq. (1), the fermion number is fixed, and $|\Phi_0\rangle$ does not have the form (4). However, one can perform a particle-hole transformation on $L/2$ sites, for example on every second one, by which the Hamiltonian acquires pair creation and annihilation terms ($B\neq 0$). Then $|\Phi_0\rangle$, which originally contains $L/2$ particles, becomes a superposition of terms with particle numbers ranging from 0 to L and can again be written in the form (4). In the same way, an arbitrary n-particle eigenstate of H could be handled by exchanging particles and holes at n sites. The density-matrix spectrum is not affected by such local transformations.

To carry out the calculation, one makes the problem formally one-dimensional by numbering the sites from 1 to L in such a way that the desired partition into two parts arises naturally. For example, a meanderlike numbering as in Ref. 26 permits a division of the square into two halves.

In Fig. 7, the single-particle eigenvalues ε_l for such a half-system and three different sizes are shown. One notices two features which are in contrast to the one-dimensional results: a ''foot'' of low-lying ε_l and a much smaller slope of the curves (note the scales). Both are strongly size-dependent. The number of ε_l in the foot is equal to N, which indicates that these states are closely connected with the interface between system and environment. Figure 8 shows the first 2000 eigenvalues w_n which result. Due to the small ε_l, they decrease very slowly and the situation worsens as the system is enlarged. The tails of the curves can be described qualitatively by $\ln(w_n)\sim-\ln^2(n)$ as in Refs. 11 and 12. The effect of these tails shows up even more in the truncation error f_n, which is defined as the sum of all w's beyond n. This quantity is given in the inset of the figure. With $n=2000$ it is approximately 5×10^{-2}, 5×10^{-1}, and 10^{-1}, respectively. Thus the situation is not only much worse than for one-dimensional systems, but also worse than for the two-dimensional system with a gap discussed in Ref. 12. Standard DMRG calculations using, say, 2000 states would be limited to sizes below 12×12, and even then the accuracy would be much less than one is used to in quantum chains.

One can also calculate the density-matrix spectra for other shapes of the selected subsystem. As an illustration, we show in Fig. 9 results for one quarter of a quadratic system (for example the upper right one). Note that the sizes indicated

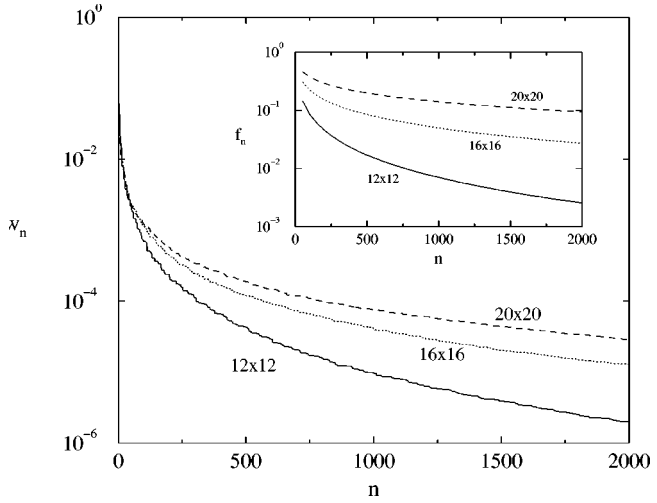

FIG. 8. Density-matrix eigenvalues w_n of two-dimensional tight-binding models, obtained from the ε_l in Fig. 7. The inset shows the truncation error (see text).

there refer to the whole system. One sees again some small eigenvalues, but fewer than for the half-system, while there are further higher-lying plateaus and additional short steps. Obviously this reflects the particular interface with a corner. For the 10×10 system, for example, the two lowest plateaus contain 9 states which is just the number of sites along the interface. The eigenvalues w_n are plotted in the inset of the figure. They are similar to those for the half-system but some more steps persist for small n. In the same way, one can investigate cases where one cuts the square diagonally at various positions. Such partitions appear in a recent new DMRG algorithm.[27] The general features of the spectra, however, do not change.

Finally, let us mention that one can also include spin in H and thereby treat the Hubbard model in the $U=0$ limit. Then the operators f_l, $f_l^\dagger$ in ρ_1 acquire a spin label, too, and all single-particle levels become doubly degenerate. This makes

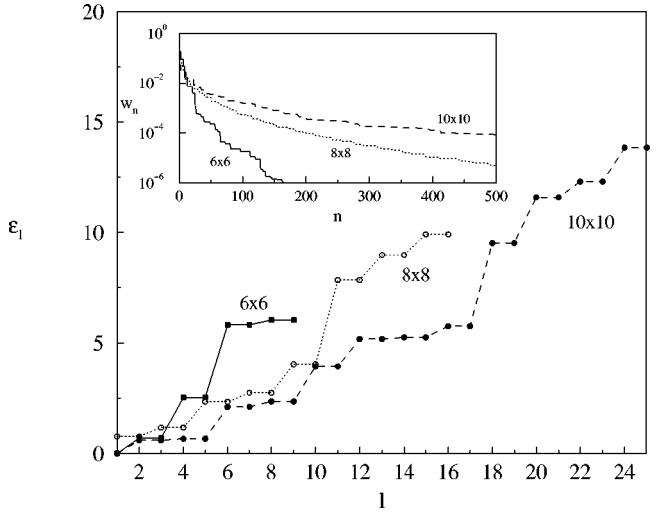

FIG. 9. Single-particle eigenvalues ε_l of two-dimensional tight-binding models. The ε_l are for a quarter of the system; the w_n obtained from them are plotted in the inset.

the tails of the w_n curves even flatter than in the spinless case. However, the curves are also pulled down by smaller normalization factors which leads to a faster initial decay. For a 20×20 lattice, the spectrum of the first 3000 states is, on the whole, rather close to that shown in Fig. 8.

VI. CONCLUSION

We have studied the reduced density matrices for noninteracting fermions on a lattice. The key ingredient for the calculation was a simple representation of the (ground) state. This led rather directly to the exponential Boltzmann-like form of the density matrices. The only really numerical step involved was the calculation of the single-fermion eigenvalues appearing in the exponent. With these, we discussed a number of cases in one and two dimensions with characteristic differences. We focused on the eigenvalues, but one can also investigate the single-fermion eigenfunctions. One then sees that they are concentrated near the interface between the two parts of the system. This explains the decisive role of the connectivity for the spectra.

One should mention that fermionic density matrices have been studied before, e.g., in quantum chemistry.[28,29] However, in this case the systems are continuous and the Hilbert space is infinite. Then already the single-particle density matrices have inifinitely many eigenstates.[30] Our systems are discrete, but we are interested in density matrices for arbitrarily large subsystems. These are non-trivial even for noninteracting fermions. From the experience with other models, one can expect that the results are roughly representative also for more complicated systems.

For this reason, the two-dimensional case is particularly important. With our formulas, we could treat the tight-binding model for arbitrary partitions of the system. This allows us to make much more detailed statements than a previous, purely numerical investigation of this system.[26] In particular, one can see the very slow decay of the spectra and of the truncation errors directly. Basically, it is connected with the existence of long boundaries between the two parts of the system. In the current DMRG procedures, these appear necessarily at some point of the calculation. Therefore it is not yet clear whether a recent algorithm[27] can really overcome this problem.

ACKNOWLEDGMENTS

We are indebted to H. Grabert who drew our attention to fermionic coherent states. M.C.C. thanks C.T. Chan for discussions and the Deutscher Akademischer Austauschdienst (DAAD) for financial support.

APPENDIX

Here we list some details concerning the steps in Sec. II. (A) To derive Eq. (7), one writes Eq. (6) explicitly as

$$\sum_n (g_{kn}c_n + h_{kn}c_n^\dagger)e^F|0\rangle = 0, \tag{A1}$$

where $F=1/2\Sigma_{ij}G_{ij}c_i^\dagger c_j^\dagger$. Using the relation

$$[c_i, e^F] = \frac{\partial}{\partial c_i^\dagger} e^F \tag{A2}$$

the exponential factor can be brought to the left

$$e^F \sum_n \left\{ \sum_m g_{km} G_{mn} + h_{kn} \right\} c_n^\dagger |0\rangle = 0. \tag{A3}$$

Since this must hold for all k, the only possibility is that the term in the bracket vanishes which gives the desired result.

(B) The explicit form of the integrand in Eq. (13) is

$$\exp\{-\xi_2^{*T}\xi_2 + 1/2(\xi_2^{*T} a^{22} \xi_2^* - \xi_2^T a^{22} \xi_2) - (\xi_1^{*T} a^{12} \xi_2^* + \xi_2^T a^{21} \xi_1') + 1/2(\xi_1^{*T} a^{11} \xi_1^* - \xi_1'^T a^{11} \xi_1')\}, \tag{A4}$$

where $\xi_1^*, \xi_1'(\xi_2^*, \xi_2)$ are vectors composed of the variables of part 1 (part 2), respectively. Using the notation $\xi \equiv (\xi_2, \xi_2^*)$, this can be rewritten as

$$\exp\{-\xi^\dagger \hat{B} \xi + \zeta^\dagger \xi + \xi^\dagger \eta + \hat{K}\}, \tag{A5}$$

where $\hat{B}$ is a $2(L-M)\times 2(L-M)$ matrix containing a^{22}, ζ, η are both $2(L-M)$ dimensional vectors constructed from a^{12}, a^{21}, ξ_1^*, and ξ_1' and $\hat{K}$ is the last term in Eq. (A4). Equation (A5) is an explicit Gaussian form which can be integrated whereby Eq. (14) is obtained.

(C) To derive the operator form for ρ_1 from Eq. (14), one first diagonalizes the matrix β. This transforms Eq. (14) into a similar form with modified matrix α. Using the relations

$$\langle \xi_i \xi_j | c_i^\dagger c_j^\dagger = \langle \xi_i \xi_j | \xi_i^* \xi_j^*, \quad c_i c_j | \xi_i', \xi_j' \rangle = \xi_i' \xi_j' | \xi_i' \xi_j' \rangle, \tag{A6}$$

one can replace $\xi_i^* \xi_j^*$ with $c_i^\dagger c_j^\dagger$ and $\xi_i' \xi_j'$ with $c_i c_j$ in the left and right exponentials. The cross terms $e^{\lambda_i \xi_i^* \xi_i'}$, where λ_i is one of the eigenvalues of β, can be rewritten with the relation

$$\langle \xi_i | f(c_i^\dagger, c_i) | \xi_i' \rangle = e^{\xi_i^* \xi_i'} f(\xi_i^*, \xi_i'). \tag{A7}$$

In our case the left-hand side equals $e^{\lambda_i \xi_i^* \xi_i'} = 1 + \lambda_i \xi_i^* \xi_i'$ so that

$$f(c_i^\dagger, c_i) = [1 + (\lambda_i - 1) c_i^\dagger c_i] = e^{\ln \lambda_i c_i^\dagger c_i}. \tag{A8}$$

Transforming back to the original representation leads to Eq. (16).

(D) The operator ρ_1 in Eq. (16) can be diagonalized by calculating the Heisenberg operators $\rho_1 c_j \rho_1^{-1}$ and $\rho_1 c_j^\dagger \rho_1^{-1}$ as in Ref. 20. Due to the form of ρ_1, they are linear combinations of the c and $c^\dagger$. Inserting the Bogoliubov transformation and following Ref. 20 one finds that the eigenvalues ε_l can be obtained from the equation

$$(\beta + \beta^{-1} + \beta^{-1}\alpha - \alpha\beta^{-1} - \alpha\beta^{-1}\alpha)\chi_l = 2\cosh \varepsilon_l \chi_l. \tag{A9}$$

Typically, the matix β has elements which vary exponentially over a large range. This limits the size of the systems for which one can use Eq. (A9) in actual numerical calculations.

[1] S. R. White, Phys. Rev. Lett. **69**, 2863 (1992).
[2] S. R. White, Phys. Rev. B **48**, 10 345 (1993).
[3] For a review, see *Density-Matrix Renormalization*, edited by I. Peschel, X. Wang, M. Kaulke, and K. Hallberg, Lecture Notes in Physics Vol. 528 (Springer, Berlin, 1999).
[4] M. Kaulke and I. Peschel, Eur. Phys. J. B **5**, 727 (1998).
[5] T. Nishino and K. Okunishi, in *Strongly Correlated Magnetic and Superconducting Systems*, edited by G. Sierra and M. A. Martín-Delgado, Lecture Notes in Physics Vol. 478 (Springer, Berlin, 1997) (see also cond-mat/9610107).
[6] R. J. Baxter, *Exactly Solved Models in Statistical Mechanics* (Academic, New York, 1982).
[7] I. Peschel, M. Kaulke, and Ö. Legeza, Ann. Phys. (Leipzig) **8**, 153 (1999).
[8] I. Peschel and M. C. Chung, J. Phys. A **32**, 8419 (1999).
[9] C. Ritter and G. von Gehlen, cond-mat/0009255 (unpublished).
[10] C. Ritter, Ph.D. thesis, Universität Bonn, 1999.
[11] K. Okunishi, Y. Hieida, and Y. Akutsu, Phys. Rev. E **59**, R6227 (1999).
[12] M.-C. Chung and I. Peschel, Phys. Rev. B **62**, 4191 (2000).
[13] E. Lieb, T. Schultz, and D. Mattis, Ann. Phys. (N.Y.) **16**, 407 (1961).
[14] *Superconductivity*, edited by R. D. Parks (Dekker, New York, 1969), Vol. 1, Chap. 2.
[15] J. W. Negele and H. Orland, *Quantum Many-Particle Systems*, Frontiers in Physics Vol. 68 (Addison-Wesley, Redwood City, CA, 1987).
[16] I. Peschel and T. T. Truong, Z. Phys. B: Condens. Matter **69**, 385 (1987).
[17] Ö. Legeza and G. Fáth, Phys. Rev. B **53**, 14 349 (1996).
[18] M. Dudziński, G. Fáth, and J. Sznajd, Phys. Rev. B **59**, 13 764 (1999).
[19] D. B. Abraham, Stud. Appl. Math. **50**, 71 (1971).
[20] C. Kaiser and I. Peschel, J. Stat. Phys. **54**, 567 (1989).
[21] See, for example, the articles by T. Nishino *et al.* and by A. Drzewiński in Ref. 3.
[22] T. T. Truong and I. Peschel, Int. J. Mod. Phys. B **4**, 895 (1990).
[23] E. Barouch and B. M. McCoy, Phys. Rev. A **3**, 241 (1971).
[24] J. Stephenson, J. Math. Phys. **11**, 420 (1970).
[25] H. Hinrichsen, K. Krebs, M. Pfannmüller, and B. Wehefritz, J. Stat. Phys. **78**, 1429 (1995).
[26] S. Liang and H. Pang, Phys. Rev. B **49**, 9214 (1994).
[27] T. Xiang, J. Lou, and Zh. Su, cond-mat/0102200 (unpublished).
[28] A. J. Coleman, Rev. Mod. Phys. **35**, 668 (1963); T. Ando, *ibid.* **35**, 690 (1963).
[29] E. R. Davidson, *Reduced Density Matrices in Quantum Chemistry* (Academic, New York, 1976).
[30] For an early picture of a spectrum (for the case of the hydrogene molecule), see E. R. Davidson and L. L. Jones, J. Chem. Phys. **37**, 2966 (1962).